applied sciences

MDPI

Article

The Biodeterioration Process in *Compositionum*: Four Ancient Multi-Material Volumes Studied by Multidisciplinary Approach

Chiara Gardenghi [1,2], Annamaria Alabiso [2,3], Marco Maria D'Andrea [2], Sara Frasca [4], Valeria Guglielmotti [5], Claudia Mazzuca [5], Noemi Orazi [6], Beatrice Ercolani [5], Stefano Paoloni [6], Alessandro Rubechini [7] and Luciana Migliore [2,8,*]

1 PhD Program in Evolutionary Biology and Ecology, University of Rome Tor Vergata, 00133 Rome, Italy; chiara.gardenghi@students.uniroma2.eu
2 Department of Biology, Tor Vergata University of Rome, Via della Ricerca Scientifica snc, 00133 Rome, Italy; annamaria.alabiso@uniroma2.it (A.A.)
3 Department of Literary, Philosophical and Art History Studies, Tor Vergata University of Rome, Via Columbia 1, 00133 Rome, Italy
4 Department of Environmental Biology, Sapienza University of Rome, Via Cesare de Lollis 21, 00185 Rome, Italy; sara.frasca@uniroma1.it
5 Department of Chemical Science and Technologies, Tor Vergata University of Rome, Via della Ricerca Scientifica 1, 00133 Rome, Italy; valeria.guglielmotti@uniroma2.it (V.G.); claudia.mazzuca@uniroma2.it (C.M.); beatrice.ercolani@uniroma2.it (B.E.)
6 Department of Industrial Engineering, Tor Vergata University of Rome, Via del Politecnico snc, 00133 Rome, Italy; noemi.orazi@uniroma2.it (N.O.); stefano.paoloni@uniroma2.it (S.P.)
7 Laboratory of Conservation, Restoration and Bookbinding, Vatican Apostolic Archive, Cortile del Belvedere, 00120 Vatican City, Vatican City State; conservazione@aav.va
8 Department of Theoretical and Applied Sciences, eCampus University, Via Isimbardi 10, 22060 Novedrate, Italy
* Correspondence: luciana.migliore@uniroma2.it

Abstract

Ancient books and documents constitute an important cultural heritage, which are composed by different supports, such as cardboard, parchment and paper. Due to their composition (animal- and plant-based matrices), they allow bacteria and fungi to thrive, causing the phenomenon of biodeterioration, an ecological succession in parchment. Four ancient books called "*Compositionum*" from the Apostolic Vatican Archive, made of the same materials, exposed to weather-beating conditions and showing different degrees of deterioration, were analysed by a multidisciplinary approach: DNA metabarcoding using NGS, Light Transmission Analysis and Raman and FTIR spectroscopy. The results highlighted how the biodeteriogen community composition changed from the least to the most damaged, without evidence of significant microbial transfer across the three matrices. The results allow confirmation of the ecological succession as biodeterioration process, including cardboard and paper, in addition to in parchment. These results give important insight for the conservation and restoration practices of all matrices.

Keywords: biodeterioration; microbial succession; DNA metabarcoding; multidisciplinary approach; Light Transmission Analysis; Raman spectroscopy; FTIR spectroscopy; conservation and restoration strategies

Academic Editors: Francesco Guarino, Agnieszka Pilarska, Pilar Garcia-Jimenez, Maria Gavrilescu and Daniele Ghezzi

Received: 19 December 2025
Revised: 17 January 2026
Accepted: 18 January 2026
Published: 21 January 2026

1. Introduction

Ancient books/archival documents constitute an important part of our cultural heritage, preserving not only irreplaceable historical, artistic and social information—the

document content—but also physical, chemical and biological data related to the document itself, as a physical object. Over time, a variety of writing supports were adopted, organized in various formats and made from different materials: among others, parchment, cardboard and paper.

Parchment is made from animal skin (typically calf, goat or sheep), so it mainly consists of collagen, a structural protein composed by a repetitive sequence of amino constituting the alpha chains, which wrap around each other to form a triple helix; the alpha sequence includes a glycine (the smallest amino acid) at every third position, which allows the three chains to pack tightly into the central core of the triple helix to form tropocollagen, which further assemble into strong, fibrous structures, providing exceptional tensile strength [1,2].

Carboard and paper are made from plant fibres (i.e., cotton, linen, wood pulp, straw, etc.) that are pulped, mixed with water, pressed into sheets, and dried, resulting in everything from thin paper to thick cardboard, depending on the pulp concentration [3]. They are composed of cellulose fibres, long chains of glucose units linked together by strong bonds, forming a complex carbohydrate (polysaccharide) without coiling or branching. Furthermore, the glucose from one chain can form hydrogen bonds with oxygen atoms on a neighbouring chain, firmly holding together the chains and forming microfibrils with high tensile strength [4].

Due to their organic composition, ancient documents constitute a source of energy and nutrients for the growth of different organisms, including bacteria and fungi, which can cause severe alterations and lead to a loss of readability, resulting from the disappearance not only of the written content, but also of the artifact. These microorganisms are known as biodeteriogens and are considered responsible for the biodeterioration, the set of chemical and physical processes induced by the activity of organisms capable of producing irreversible loss of value and/or information in the writing substrates [5,6]. The activity of these microbial biodeteriogens can be considered part of the natural large scale processes allowing the recycling of nutrients (the bio-geo-chemical cycles) [7], in which they play the pivotal role of decomposers/consumers (with insects and other animals) in environments rich in organic matter, such as dung, carcasses, or leaf litter. In these decomposition processes, chemical energy is high at the start and declines as organic material is broken down and are nutrients recycled, a process called heterotrophic succession [7].

The heterotrophic succession involved in parchment biodegradation starts with the pivotal and pioneer role of halophilic archaea, followed by bacteria and fungi [8–10]. Previous studies unveiled the dynamic of biodegradation: a two-phase successional model, pioneered by the action of halophilic archaea and *Gammaproteobacteria*, and completed by environmental bacteria and fungi. *Halobacterium salinarum* (halophilic archaea) was identified as the main organism responsible for both the initial attack to collagen fibres and the appearance of purple spots after their collapse, due to the persistence of bacteriorhodopsin and bacterioruberin in the parchment, which are constitutive pigments of the haloarchaea [9]. Very often the archaeal DNA is not found in the samples, even if appropriate primers pairs were used (as in this study), because it can be "eaten" by subsequent colonizers. Therefore, its presence is confirmed by the production of purple spots, which depends on the collapse of the archaeal cells [8–10]. Conversely, limited information is available in the literature on the deterioration process involving cardboard and paper as components of a book, although some microbial colonizers were identified on these matrices [11–14].

Historical books are often complex multi-material artifacts, as the '*Compositionum*' volumes, belonging to a collection stored in the Apostolic Vatican Archives (ex-Secret Vatican Archive, Vatican City), dated 1807. These books were registers of the Vatican *Prefectus Compositionum* office, responsible for receiving and managing the payments of

graces and dispensation. They are four volumes presenting a semi-limp parchment binding with a parchment book cover, bearing boards made of flexible paper cardboard and closed by three alum-tawed skin strips, including a paper text block; all volumes are made in the same way, as to allow a possible attribution to the same hand and let us to suppose that were made of the same kind of materials. The volumes were exposed to the same deterioration agent, weathering (probably rainfall), but display a different degree of deterioration, that we classified from the least to the most damaged in a scale from 1 to 4 (Figure 1).

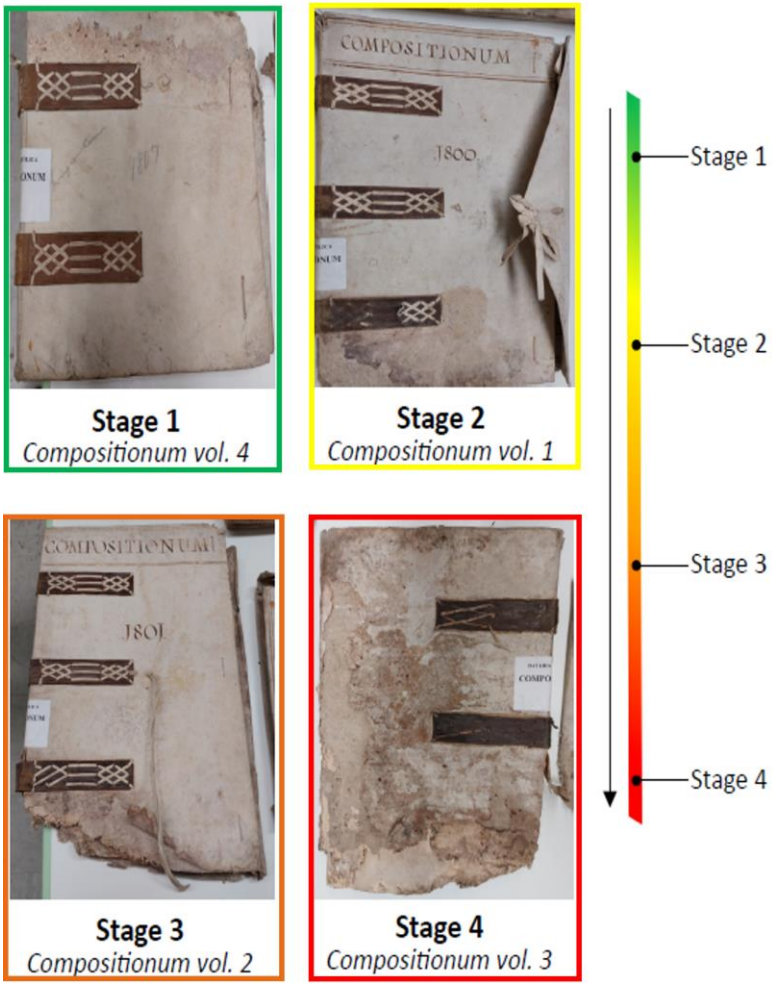

Figure 1. The four volumes of the *Compositionum* ordered according to their relative conservation status (from the Apostolic Vatican Archive, Vatican City; Photos by A. Alabiso).

To evaluate the dynamics that occurred in each matrix of these multi-material books, a multidisciplinary approach was used, combining the following: (i) *16S rRNA*/ITS2-5.8 rDNA gene metabarcoding using Next Generation Sequencing to obtain the taxonomical identification of bacterial and fungal biodeteriogens in the different matrices; (ii) Light Transmission Analysis (LTA) to evaluate the hydrothermal stability of the parchment collagen—a proxy of its degradation rate—in the four degradation stages; (iii) Raman spectroscopy to identify the pigments staining the biodeteriorated areas, and finally, (iv) FTIR spectroscopy to evaluate the presence of animal glue in the cardboard and paper.

The aim of this study was to identify the main actors of the biodegradation process, to clarify the degradation dynamics in the different matrices and to evaluate the possible biodeteriogen transfer between matrices, due to their physical proximity.

2. Materials and Methods

2.1. Sample Collection and Damage Evaluation

Four ancient volumes dated 1807 and called *Compositionum* were chosen among the wide collections of the Apostolic Vatican Archive (ex-Secret Vatican Archive). The books (Figure 1) are all made of different matrices (semi-limp parchment binding with a parchment book cover, paper cardboard, paper text block and three alum-tawed skin strips to close the binding on the fore edge). All the volumes were subjected to the same degradation agent, probably rainwater, but they show a different degree of degradation: in Table 1 the volumes' deterioration rate is reported for each book matrix from the least damaged, classified as 1, to the most damaged, classified as 4, as already shown in Figure 1.

Table 1. Evaluation of the volumes' deterioration for each book matrix. PC = parchment; CB = cardboard; and PR = paper.

Volume nr.	Sample ID	Conservation	Matrix	Observed Damages
4	PC_S1	Stage 1	Parchment	Purple spot slight deterioration
	CB_S1	Stage 1	Cardboard	Aged matrix
	PR_S1	Stage 1	Paper	Aged matrix
1	PC_S2	Stage 2	Parchment	Purple spot deterioration
	CB_S2	Stage 2	Cardboard	Brown spots
	PR_S2	Stage 2	Paper	Brown spots
2	PC_S3	Stage 3	Parchment	Purple spot severe deterioration
	CB_S3	Stage 3	Cardboard	Extensive brown spot discolouration
	PR_S3	Stage 3	Paper	Brown spot severe discolouration
3	PC_S4	Stage 4	Parchment	Purple spot severe deterioration Holes and rips
	CB_S4	Stage 4	Cardboard	Severe brown spot discolouration Holes and rips
	PR_S4	Stage 4	Paper	Severe brown spot discolouration Holes and rips Pages compaction

From each of the four volumes, small pieces of each matrix (about 2–8 mm^2 each), already detached and impossible to be relocated during the restoration process, were collected in triplicate in sterile conditions.

2.2. Identification of Microbial Colonizers by 16S and ITS2-5.8S rDNA Gene Analysis

2.2.1. DNA Metabarcoding

To evaluate the presence of bacterial and fungal strains in the different books and matrices, each sample was processed to extract metagenomic DNA, using the Power Soil®DNA isolation kit (Mo Bio, Carlsbad, CA, USA), according to the manufacturer's instructions. The bacterial rDNA gene region *16S rRNA* (variable region V4) was amplified by the primers 515F (forward, 5′-GTGCCAGCMGCCGCGGTAA-3′) and 806R (reverse, 5′-GGACTACHVGGGTWTCTAAT-3′), which are prokaryotic universal primers for simultaneous analysis of bacteria and archaea [15]. The conditions for PCR amplification were as follows: a denaturation step at 94 °C for 3 min, then 28 cycles of 94 °C for 30 s, 53 °C for 40 s and 72 °C for 1 min, with a final extension step of 72 °C for 5 min. The fungal rDNA gene region ITS2-5.8S was amplified using the ITS3-mixF (forward, 5′-CAWCGATGAAGAACGCAG-3′) and ITS4R (reverse, 5′-TCCTCCGCTTATTGATATGC-3′) primers [16,17]. The conditions for PCR amplification were as follows: a denaturation step at 95 °C for 15 min, then 35 cycles of 95 °C for 30 s, 54 °C for 40 s and 72 °C for 1 min, with a

final extension step of 72 °C for 10 min. Both amplicon products were checked using a 1.5% and 0.8% agarose gel, respectively. For the purification of PCR products, the MiniElute PCR purification kit (Qiagen, Venlo, The Netherlands) was used following the manufacturer's instructions. The samples were sent to Eurofins Genomics (Ebersberg, Germany) to be processed by Illumina paired-end NGS.

2.2.2. Bioinformatic Analyses

Raw reads were processed using the QIIME 2 (Quantitative Insights Into Microbial Ecology v2022.2) platform [18]. Sequences were filtered, denoised and checked for chimeras using the DADA2 pipeline [19] to obtain Amplicon Sequences Variant (ASV) tables.

The quality filtering thresholds for DADA2, processing forward and reverse reads, were set to the following: 180 and 130 for bacterial sequences and 250 and 200 for fungal sequences.

Taxonomic identification of bacterial *16S rRNA* sequences was performed by using a Naive Bayes classifier trained on the SILVA 138 SSU database [20], while for fungal ITS2-5.8 rDNA sequences, a classifier trained on the UNITE database 8.3 version was used [21]. ASVs were clustered into Operational Taxonomic Units (OTUs) using the q2-vserach plugin, with a 97% similarity threshold for bacteria and a 99% similarity threshold for fungi. Subsequently, both bacterial and fungal OTU tables and sequence files were filtered to remove mitochondria, chloroplast and unclassified entries by using the QIIME 2 taxa filter-table and filter-seqs tools, respectively. Normalization was finally performed using the q2-srs plugin, rarefying each dataset to the lowest sequencing depth observed (11,773 reads for bacteria, corresponding to sample PC_S1_3, and 38,031 reads for fungi, corresponding to sample PC_S4_2).

Diversity analyses were performed on the normalized datasets using QIIME 2 v2022.2. Alpha and beta diversity indices were used to measure species diversity in single samples and their differences between samples. Specifically, alpha diversity was quantified by Shannon's diversity index (H'), while beta diversity was quantified by the Bray–Curtis and Unweighted UniFrac distance matrices. The statistical significance of the differences was checked by the Kruskal–Wallis test for alpha diversity and the PERMANOVA test for beta diversity, by using 9999 permutations.

The sequences classified with QIIME 2 v2022.2 were further analysed to evaluate the putative ecological functions of bacterial OTUs, using FAPROTAX v1.2.7, and to focus on the putative trophic or metabolic function of fungal OTUs, using FUNGuild v1.0 [22,23], in the three matrices of each book and degradation stage.

2.3. Characterization of the Animal-Based Matrix, the Parchment

2.3.1. Parchment Stability Evaluation by Light Transmission Analysis

To measure the hydrothermal stability of collagen in the parchment samples, a dedicated technique, Light Transmission Analysis (LTA), was used with visual control by microscopy [24]. Each parchment sample (approx. 1 mm^2) was cut and placed in water to create a pulp by using a blade. Then each sample was put into a 0.1 mm thick quartz cell under a He–Ne laser beam (λ = 633 nm), whose temperature varied with a constant temperature rate of about 1 °C/min up to 90 °C. The sample temperature is continuously recorded to evaluate the denaturation temperature, T_d, which corresponds to the temperature where the maximum change in the signal amplitude (L) of the transmission light—and therefore in the denaturation activity—occurs. At T_d, the LTA curves therefore show a peak. Often, collagen-based material shows more than a single peak, revealing the presence of different collagen fractions, in terms of chemical stability. In the case of the parchment samples, LTA denaturation curves typically show two distinct peaks (see Figures S1–S8 in

the Supplementary Materials). The first peak (T_N) can be associated with the *native collagen* fraction, which is located in the core of the parchment fibre and is less structured, while the second peak (T_S) can be associated with the *stabilized collagen* fraction, which is located in the outer sheath of the fibre and has a higher denaturation temperature [24,25]. In this work the progressive variation in stability during the different stages was evaluated by analysing the denaturation temperature behaviours.

All measurements were performed in triplicate and for statistical analyses GraphPad Prism 8.0.2 for Windows (GraphPad Software, San Diego, CA, USA) was used to evaluate differences among and between the deterioration stages by using Kruskal–Wallis test and one-way ANOVA test with Tukey's HSD *post-hoc* pairwise comparisons.

2.3.2. Chemical Identification of Discoloured Areas by Raman Spectroscopy and UV–Vis Absorption

Raman spectroscopy is a non-destructive technique used that allows for the identification of the chemical composition of the discoloured areas of damaged documents. This technique was firstly performed directly on a small piece of each sample by using the HORIBA LabRam Odyssey spectrometer (Palaiseau, France) with a laser source of 532 and 785 nm.

Then, chemical extraction was performed on samples from stages 1, 2, 3 and 4, by using three different solvents for the extraction of water-soluble pigments, lipophilic pigments and insoluble melanin, i.e., distilled water and cyclohexane for polar and apolar substance extraction, respectively. Each weighed sample (approximately 9 mg) was immersed into the solvent and subjected to extraction with the aid of an ultrasonic bath heated to approximately 50 °C for 1 h. Each supernatant was than tested by UV–Vis absorption spectroscopy, in the range 300–700 nm.

For melanin extraction, a modified protocol [26] was used: Each sample (about 9 mg) was immersed in 5 mL of NaOH 1M solution, kept at a temperature of 120 °C (in water bath) for 20 min, to facilitate the solubilization of melanin. The solutions were then centrifuged (1800× *g* (RCF); 5 min) to collect the supernatant fraction containing the dissolved melanin. Absorption spectra of both the extracted samples and the reference NaOH solution were registered in the range 300–700 nm. To obtain the melanin precipitation, 5 mL of HCl 1 M were added to each supernatant and centrifuged at ≈1800× *g* (RCF) for 5 min.

2.4. Characterization of the Plant-Based Matrices, the Cardboard and Paper

2.4.1. Cardboard and Paper Characterization

Lignin content. Graff C stain [27] was used to estimate cardboard and paper fibre composition. Graff C reactive stain was prepared by mixing it in 52 mL of a $ZnCl_2$ saturated solution, with 0.06 mol of $AlCl_3$, 0.06 mol of $CaCl_2$, 0.64 mmol of I_2 and 1.4 mmol of KI, which was dropped on the samples.

The phloroglucinol colorimetric reagent was used to evaluate the presence of lignin: a solution of 1.00 g phloroglucinol in 50 mL of ethanol and 25 mL of 37% hydrochloric acid. A drop of the solution was applied on the carboard and paper samples to check for a reaction with lignin, and the consequent colour development induced by the reaction [28].

Potential of hydrogen (pH). A Crison Instrument (mod. Basic-20, Crison Instrument s.a., Alella, Barcelona, Spain) and a flat tipped symmetry glass electrode (Hanna Instrument., Woonsocket, RI, USA) was used to measure the pH of the cardboard and paper sample surfaces.

Protein content. A Bradford assay was used to evaluate the presence of animal glue, a drop of Bradford reagent was applied directly on the sample: the dye binds to proteinaceous materials and produces a blue colour shift, allowing the detection of animal glue or gelatine-based sizing [29].

All reagents have been purchased by Merck (Merck KGaA, Darmstadt, Germany) and used without further purification.

2.4.2. Chemical Identification of Sizing Glue by FTIR Spectroscopy

A Nicolet iS50 Thermo Scientific instrument (Thermo Scientific Inc., Madison WI, USA) equipped with a single reflection diamond Attenuated Total Reflectance (ATR) cell (Everest Diamond ATR accessory) was used to obtain FTIR spectra by analysing non-replaceable fragments of the four volumes. Spectra were recorded in the wavenumber's region from 4000 to 550 cm^{-1}, averaging at least 32 scans with a resolution of 4 cm^{-1}.

3. Results

3.1. Bacterial Colonizers

3.1.1. Bacterial Community Composition and Diversity

Bioinformatic analysis, performed with QIIME 2, identified a total of 756,608 bacterial sequences, divided for matrix and degradation stage, as reported in Table 2. In this set, 6160 ASVs were identified, which were clustered into 507 OTUs (97% of similarity by the DADA2 plugin).

Table 2. Bacterial sequences identified in the three matrices of the *Compositionum* volumes, according to the degradation stage (N = 36). In brackets, the percentage of the total amount of bacterial sequences.

Matrix	Number of Sequences			
	Stage 1	**Stage 2**	**Stage 3**	**Stage 4**
Parchment	53,070 (7.01%)	78,169 (10.33%)	87,546 (11.57%)	61,389 (8.11%)
Cardboard	45,128 (5.96%)	70,184 (9.28%)	59,163 (7.82%)	68,082 (9.00%)
Paper	64,924 (8.58%)	55,843 (7.38%)	57,171 (7.56%)	55,939 (7.39%)

As expected, the three matrices harboured bacterial communities with significantly different alpha-diversity (Kruskal–Wallis test, $p = 0.0001$). The comparison showed a significant difference between parchment ($H' = 4.49 \pm 1.22$) and both cardboard ($H' = 7.20 \pm 0.55$) and paper ($H' = 6.76 \pm 1.37$; Kruskal–Wallis pairwise comparisons, $p = 0.0001$), while no significant difference between cardboard and paper was found ($p = 0.862$). Alpha-diversity changed along the degradation process, as reported in Table 3; there is a significant difference within the four stages in both parchment and paper (Kruskal–Wallis test, $p = 0.016$ and $p = 0.024$, respectively), while in cardboard no significant differences were found (Kruskal–Wallis test, $p = 0.063$).

The comparison among the three matrices highlighted significant differences in beta-diversity (PERMANOVA test, Bray–Curtis: pseudo-F = 4.806, $p = 0.0001$; Unweighted UniFrac: pseudo-F = 6.862, $p = 0.0001$). In addition, the Bray–Curtis pairwise comparison of bacterial communities between the three matrices highlighted statistically significant differences, as reported in Table 4. These differences also account for the different number of taxa globally found in the three matrices: 27 in parchment, 36 in cardboard and 54 in paper.

Table 3. Bacterial community diversity in the three matrices of the *Compositionum* volumes according to their degradation stage (N = 36).

Matrix	Stage	Shannon Index (Mean H′ ± SD)	Kruskal–Wallis Test
Parchment	1	3.11 ± 0.28	$p < 0.05$
	2	4.12 ± 0.04	
	3	4.41 ± 0.04	
	4	6.33 ± 0.04	
Cardboard	1	7.49 ± 0.06	n.s.
	2	7.60 ± 0.07	
	3	7.40 ± 0.39	
	4	6.33 ± 0.09	
Paper	1	5.70 ± 0.76	$p < 0.05$
	2	8.15 ± 0.25	
	3	7.92 ± 0.04	
	4	5.31 ± 0.15	

Table 4. Pairwise Bray–Curtis dissimilarity (*p*-value) of bacterial communities in parchment, cardboard and paper matrices.

	Parchment	Cardboard	Paper
Parchment	--	$p = 0.0001$	$p = 0.0003$
Cardboard	$p = 0.0001$	--	$p = 0.0001$
Paper	$p = 0.0003$	$p = 0.0001$	--

Furthermore, bacterial communities (PCoA plot in Figure 2) highlighted how the cardboard microbial community is homogeneous and distinct from those of parchment and paper matrices.

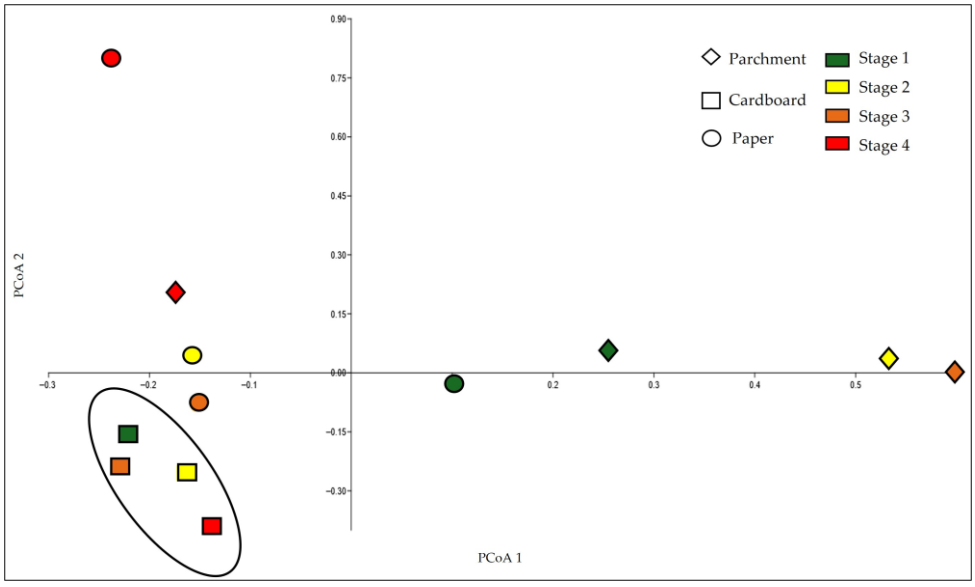

Figure 2. PCoA plot of bacterial communities, collapsed at the order level, in the three matrices of the *Compositionum* volumes, according to their degradation stage (based on Bray–Curtis distances of 36 bacterial communities, collapsed at the order level). The cardboard communities are included in the ellipse.

3.1.2. Taxonomic Identification of Bacterial Colonizers

Among the 507 OTUs, 14 phyla were detected with *Actinobacteriota*, *Pseudomonadota* and *Bacillota*, which were dominant and distributed in all samples at all stages. *Actinobacteriota*

was the most abundant phylum in parchment: 99.46% (stage 1), 99.18% (stage 2) and 97.13% (stage 3), while at stage 4 its abundance sharply decreased (12.57%) and *Pseudomonadota* became dominant (70.34%). *Pseudomonadota* were also present in cardboard and paper, although at a low percentage: in cardboard it was <2% in the first three stages and rose to 11.52% in stage 4; in paper it was 2.68% at stage 1, 17.69% at stage 2, 7.94% at stage 3 and 17% at stage 4. *Bacillota* were found in parchment samples at low abundance: <2% (stages 1 and 2) and 2.47% and 5.82% (stages 3 and 4), while it was dominant in cardboard samples across the four stages (93.24%, 87.12%, 98.18% and 67.24%, respectively). In paper this phylum was uniformly present in the first two stages (at 33.61% and 38.96%, respectively) while its presence increased in stage 3 (61.92%) only, to be reduced to 8.99% in stage 4.

As a total, sixty-six orders were detected in all matrices (Figure 3). In parchment, *Pseudonocardiales* was the dominant taxon in the first three stages (93.09%, stage 1; 92.49%, stage 2; 92.47%, stage 3) while in stage 4 it shrunk dramatically (7.47%); *Pseudonocardia* and *Saccharopolyspora* were the most abundant genera (55% and 45%, respectively). In cardboard, *Pseudonocardiales* relative abundance was low (<2%) in stage 1 and stage 3, but higher at stage 2 and stage 4 (10.12% and 17.96%, respectively). Conversely, in paper *Pseudonocardiales* were abundant in stage 1 (58.60%), decreasing to 17.01% and 18.77% in stages 2 and 3, respectively, and falling to <2% in stage 4. The order *Xanthomonadales* was present in parchment only at stage 4 (37.94%) and scarcely represented in cardboard (<2%) and paper (3.49% and 3.95% in stages 2 and 4, respectively). Overall, *Bacillales* was rare in the parchment: <2% at stages 1–2 and 2.21 and 4.96% at stages 3 and 4, respectively. In cardboard, *Bacillales* was spread in all stages, where the highest percentages were found at stages 1 and 4 (43.05 and 49.01%, respectively); at stages 2 and 3 its relative abundance was lower (19.30 and 25.59%, respectively). Even on paper, its relative abundance was rather low, particularly in stages 1 and 4 (7.51 and 5.56%, respectively), with a slight increase in stages 2 and 3 (12.69 and 30.23%, respectively). In paper, *Sphingobacteriales* was also present, particularly at stage 4 (66.84%), while it was absent/barely represented in parchment and cardboard (3.94% in parchment, stage 4). Lastly, *Clostridiales* was absent in parchment, barely represented in paper (6% in all stages), and quite abundant in cardboard (49% in all stages).

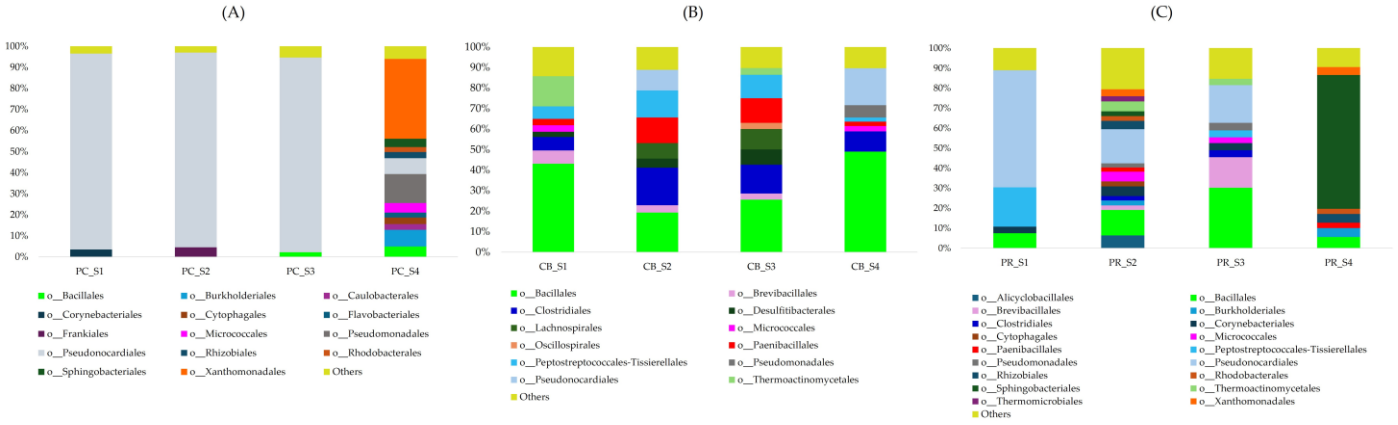

Figure 3. Composition of the bacterial communities in the three matrices: relative abundance (%) of bacterial OTUs at order level in parchment ((**A**) = PC_# samples), cardboard ((**B**) = CB_# samples) and paper ((**C**) = PR_# samples). The taxa are stacked in the same order in the figures as in the keys. 'Others' include all taxa found with a percentage < 2%.

3.2. Fungal Colonizers

3.2.1. Fungal Community Composition and Diversity

Bioinformatic analysis identified a total of 2,017,655 fungal sequences, divided for matrix and degradation stage, as reported in Table 5. Among these, 3765 ASVs were detected, which clustered into 662 OTUs (97% of similarity by the DADA2 plugin).

Table 5. Fungal sequences identified in the three matrices of the *Compositionum* volumes, according to their degradation stage (N = 36). In brackets, the percentage of the total amount of fungal sequences.

Matrix	Number of Sequences			
	Stage 1	**Stage 2**	**Stage 3**	**Stage 4**
Parchment	156,373 (7.75%)	186,480 (9.24%)	162,282 (8.04%)	139,941 (6.94%)
Cardboard	212,544 (10.53%)	162,627 (8.06%)	157,138 (7.79%	168,656 (8.36%)
Paper	176,368 (8.74%)	172,211 (8.54%)	156,849 (7.77%)	166,186 (8.24%)

As in the case of bacterial diversity, the three matrices harboured fungal communities with significantly different overall alpha-diversity (Kruskal–Wallis test, $p = 0.0001$). Pairwise comparison showed a significant difference between parchment ($H' = 3.93 \pm 1.01$), and both cardboard ($H' = 5.51 \pm 1.59$; Kruskal–Wallis, $p = 0.024$) and paper matrices ($H' = 6.70 \pm 0.95$; Kruskal–Wallis, $p = 0.000032$), while a less significant difference between cardboard and paper were found ($p = 0.049$). Alpha-diversity changed along the degradation process: as reported in Table 6, there was a significant difference within the four stages in cardboard matrices (Kruskal–Wallis test, $p = 0.0188$), while there was no significant difference in parchment and paper matrices (Kruskal–Wallis test, $p = 0.0987$ and $p = 0.0861$, respectively).

Table 6. Fungal community diversity in the three matrices of the *Compositionum* volumes according to their degradation stage (N = 36).

Matrix	Stage	Shannon Index (Mean H′ ± SD)	Kruskal–Wallis Test
Parchment	1	2.46 ± 0.16	n.s.
	2	4.53 ± 0.43	
	3	4.15 ± 0.93	
	4	4.57 ± 0.39	
Cardboard	1	3.27 ± 0.87	$p < 0.05$
	2	6.36 ± 0.23	
	3	7.06 ± 0.26	
	4	5.37 ± 0.95	
Paper	1	7.32 ± 0.79	n.s.
	2	6.72 ± 0.92	
	3	5.50 ± 0.35	
	4	7.29 ± 0.40	

The comparison among the matrices highlighted significant differences in beta-diversity (PERMANOVA test, Bray–Curtis: pseudo-F = 4.951, $p = 0.0001$; Unweighted UniFrac: pseudo-F = 1.728, $p = 0.0003$). The Bray–Curtis pairwise comparison of fungal communities between the three matrices highlighted statistically significant differences, as reported in Table 7. These differences account for the different number of taxa globally found in the three matrices: 26 in parchment, 44 in cardboard and 52 in paper.

Table 7. Pairwise Bray–Curtis dissimilarity (*p*-value) of fungal communities in parchment, cardboard and paper matrix.

	Parchment	Cardboard	Paper
Parchment	--	$p = 0.0001$	$p = 0.0001$
Cardboard	$p = 0.0001$	--	$p = 0.0032$
Paper	$p = 0.0001$	$p = 0.0032$	--

Furthermore, fungal communities (PCoA plot in Figure 4) on the parchment are clearly separated from those of cardboard and paper matrices.

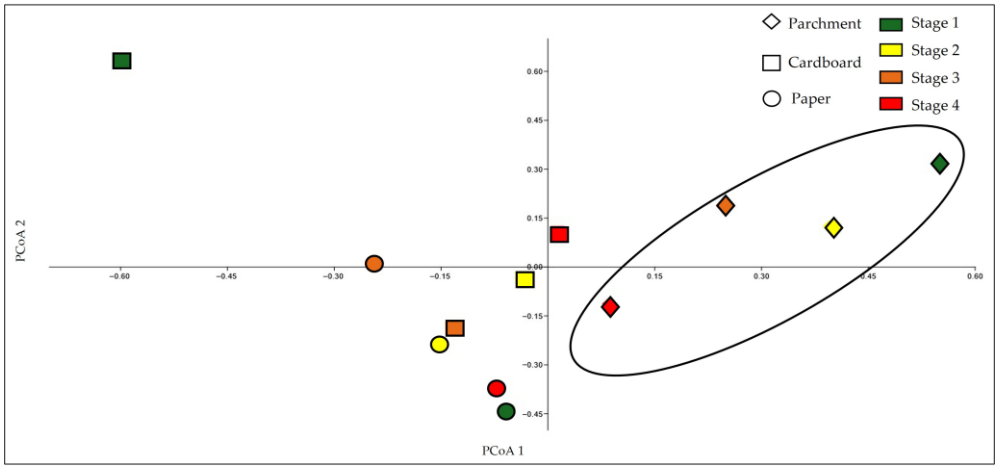

Figure 4. PCoA plot of fungal communities, collapsed at the order level, in the three matrices of the *Compositionum* volumes according to their degradation stage (based on Bray–Curtis distances of 36 fungal communities, collapsed at the order level). The parchment communities are included in the ellipse.

3.2.2. Taxonomic Identification of Fungal Colonizers

Among the 662 OTUs, two phyla were detected: *Ascomycota* and *Basidiomycota* (Figure 5). Ascomycota was the most abundant, widespread in all samples and at every stage. In parchment samples it was dominant in almost all stages, representing 100% (stage 1), 89.75% (stage 2), 95.41% (stage 3) and 98.44% (stage 4). In addition, in cardboard samples, its relative abundance was high, representing 93.76% (stage 1), 78.80% (stage 2), 62.51% (stage 3) and 85.84% (stage 4). In paper, its relative abundance was 45.87% (stage 1), 51.13% (stage 2), 74.81% (stage 3) and returned to 46.26% (stage 4). Conversely, *Basidiomycota* was always rare, particularly in parchment samples, where it was absent in stage 1 and showed a low relative abundance in the other stages: 4.05%, 4.35% and <2%, at stages 2, 3 and 4, respectively. In cardboard its relative abundance ranged from 6.12% (stage 1), to 17.51% (stage 2), to 37.49% (stage 3), returning to 13.95% (stage 4). In paper, its relative abundance was much higher: 53.86% (stage 1), 48.87% (stage 2), 53.18% (stage 4), but reduced to 24.74% at stage 3.

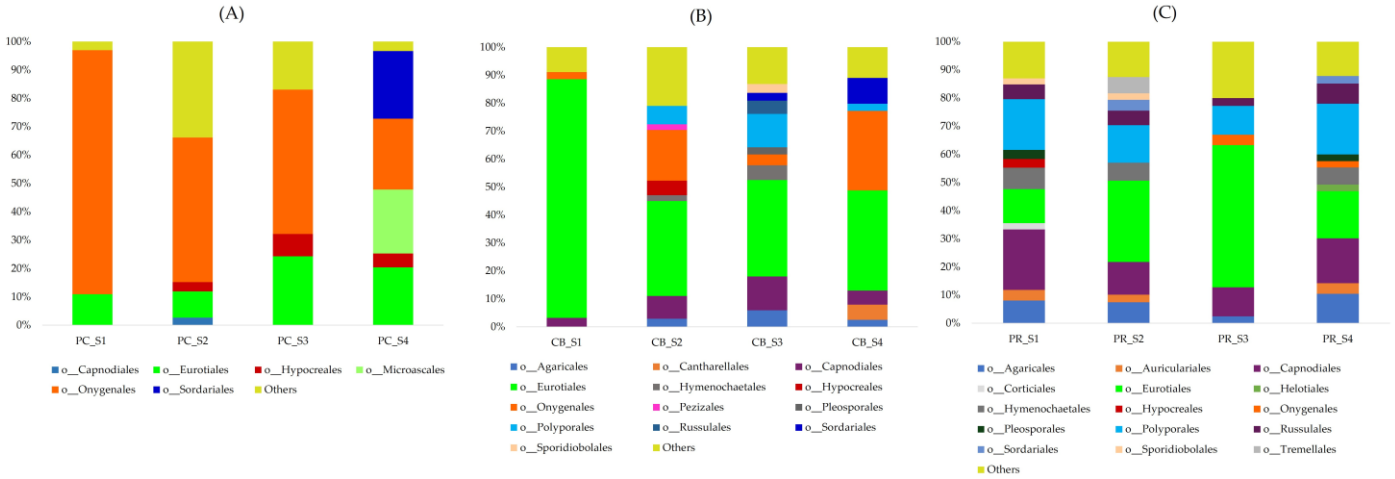

Figure 5. Composition of the fungal communities in the three matrices: relative abundance (%) of bacterial OTUs at order level in parchment ((**A**) = PC_# samples), cardboard ((**B**) = CB_# samples) and paper ((**C**) = PR_# samples). The taxa are stacked in the same order in the figures as in the keys. 'Others' include all taxa found with a percentage < 2%.

In total, forty-nine orders were detected in all matrices (Figure 5). In parchment, *Onygenales* was dominant in stage 1 (85.35%), quite high in stages 2 and 3 (51.16% and 51.14%, respectively) and reduced at stage 4 (25%). In cardboard, its relative abundance was low at stages 1 and 3 (2.58% and 3.89%, respectively) and a little higher in stages 2 and 4 (18.05% and 28.46%, respectively). In paper, its relative abundance was even lower: <2% at stages 1 and 2, 3.71% at stage 3 and 2.19% at stage 4. Parchment hosted *Microascales* and *Sordariales* (23% and 24%, respectively) only at stage 4, while in the other two matrices these orders were substantially lower (overall 2% on cardboard and paper, 14% on cardboard and 8% on paper, respectively). Even *Eurotiales* were quite rare in parchment: 10.82% and 9.23% (stages 1 and 2, respectively), while increasing with matrix degradation to 24.39% and 20.39% (stages 3 and 4, respectively). In cardboard, its relative abundance was the highest in stage 1 (85.39%), then they decreased to 33.94% (stage 2), 34.47% (stage 3) and 35.89% (stage 4). The genus *Aspergillus* was the most abundant in all the stages, representing 98% of the order *Eurotiales*. On paper, the maximum abundance of the latter genus was 50.49% in stage 3, while it was lower in stages 1, 2 and 4 at 12.13%, 28.86% and 16.68%, respectively. Finally, *Capnodiales* was present in all matrices with different abundances: it was almost absent in parchment (overall 5% in all stages), increased in cardboard (not exceeding 30% in all stages and was well represented in paper (up to 60% in all stages).

3.3. Parchment Stability Evaluation by Light Transmission Analysis

The denaturation analysis of the collagen, performed on unstained and stained areas of the parchment matrix in all four stages, highlighted differences between the areas. It is worth noting that for the most deteriorated samples the highest temperature peak (T_S) is in some cases characterized by a wide dispersion of the values obtained from repeated measurements and in some individual measurements was even undetectable. On the other hand, the observed T_S variations correspond qualitatively to those of the main peak, which is more stable and reproducible. For this reason, the analyses focused exclusively on the behaviour of T_N, evaluating the progressive changes in native collagen in the different stages, considering them the most meaningful indicator of the sample stability changes.

As reported in Table 8, the denaturation temperature regularly decreased in unstained areas through the stages, whereas in stained areas the reduction of denaturation temperature was continuous from stage 1 to stage 3 with a rise at stage 4.

Table 8. Denaturation temperature of the parchment matrix (°C) in the *Compositionum* volumes, according to their degradation stage in unstained or stained areas (N = 24).

Area	Denaturation Temperature in °C (Mean ± SD)			
	Stage 1	Stage 2	Stage 3	Stage 4
Unstained	56.07 ± 1.47	49.90 ± 0.17	47.97 ± 0.57	46.27 ± 1.40
Stained	55.77 ± 1.80	49.70 ± 0.55	48.27 ± 0.85	50.30 ± 1.80

This different dynamic in the samples is sustained by statistical analyses. In the unstained areas, there was a significant difference between the four degradation stages (one-way ANOVA, F = 48.77 and = 0.000017; Kruskal–Wallis test, $p = 0.0181$) and pairwise comparison showed a significant difference between stages 1 and 2 (Tukey's pairwise, $p = 0.0005$), stages 1 and 3 ($p = 0.0001$), stages 1 and 4 ($p < 0.001$) and stages 2 and 4 ($p = 0.0128$). No significant differences were found between stages 2 and 3 ($p = 0.1941$) and stages 3 and 4 ($p = 0.2769$), due to the slight but progressive decrease of denaturation temperature. In addition, in the stained areas there was a significant difference between the stages of degradation (one-way ANOVA, F = 17.2 and $p = 0.00075$; Kruskal–Wallis test, $p = 0.0357$), and pairwise comparisons highlighted significant differences between stages 1 and 2 (Tukey's pairwise, $p = 0.0028$), stages 1 and 3 ($p = 0.0007$) and stages 1 and 4 ($p = 0.0054$). As in unstained areas, no significant differences were found between stages 2 and 3 ($p = 0.599$), stages 2 and 4 ($p = 0.9478$); however, no significant difference was also found between stages 3 and 4 ($p = 0.3333$), with the latter showing a slight unexpected increase in T_d.

3.4. Chemical Identification by Raman and UV–Vis Absorption Spectroscopy

Raman spectra of untreated samples exhibited a strong fluorescence at 532 nm; this is a typical sinusoidal disturbance, overlapping the photoluminescence (PL) at 1574 cm^{-1} and at 2865 cm^{-1}, which could be attributed to the stretching of C=C from conjugated or aromatic species and at C–H stretching vibrations from aliphatic groups. These data did not allow for identification of the chemical species, but the spectra seemed analogous to those of melanin samples, in both Raman and PL (Figure S9 in Supplementary Materials) [30,31]. Hence, to confirm this pigment likeness, sampled were extracted under basic pH and high temperature: In Figure 6A, parchment samples from stages 1 to 4, show colours ranging from yellowish orange to brown, with the stage 2 sample displaying the most intense colour. A further acidification/centrifugation step allowed for separation of the solid melanin residue from the supernatant, but only for the stage 2 sample, which is shown in Figure 6B. Absorption spectra of all the extracted samples and the reference NaOH solution, were registered in the range 300–700 nm (Figure 6C). All the samples showed increased absorption towards the low wavelengths, with the highest value shown by the stage 2 sample. These absorption spectra are consistent with those already reported for basically solubilized melanin [26]. The extraction procedure and subsequent precipitation, together with spectroscopic data, strongly support the presence of melanin in each sample, in particular in the stage 2 sample, that results to be the richest. No other pigments were extracted with water or lipophilic solvent, but the presence of other coloured species at lower concentrations cannot be ruled out.

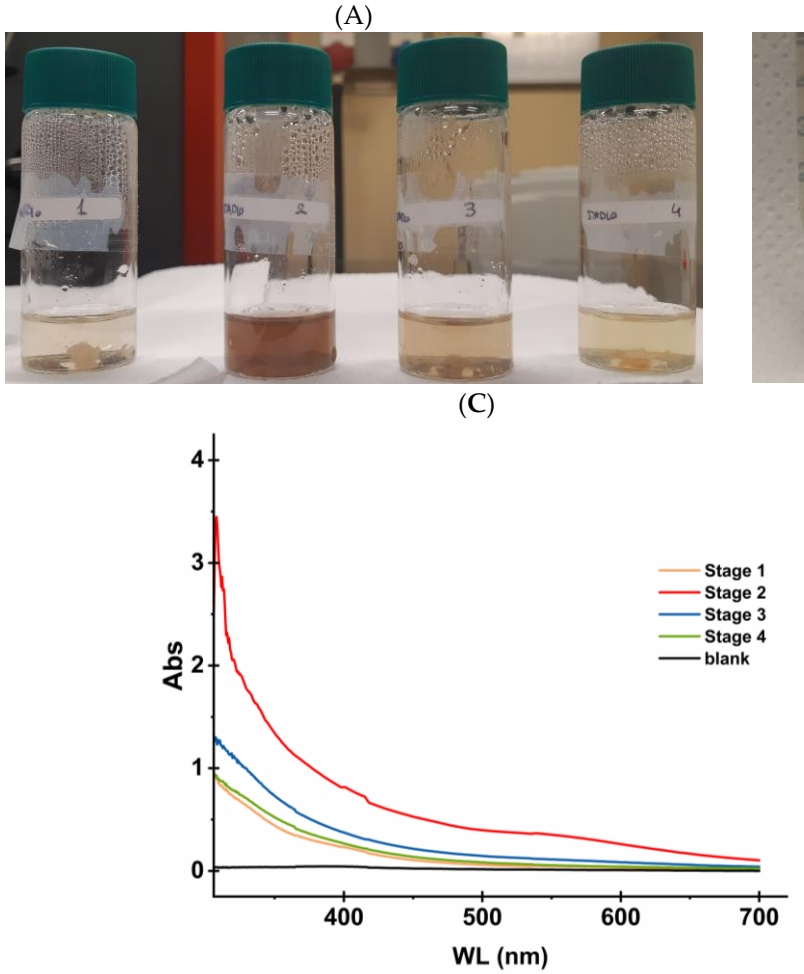

Figure 6. (**A**) Parchment samples from stages 1 to 4, dissolved under basic pH and heating treatment; (**B**) melanin precipitation after acidification in the stage 2 sample; and (**C**) absorption spectra of extracted samples of the four stages and blank (NaOH).

3.5. Cardboard and Paper Characterization by FTIR Spectroscopy and Other Spot Tests

The plant-based composition of cardboard was indicated both by the envelope of the absorption band, in the interval 1200 and 950 cm^{-1} (Figure 7A), showing the characteristic features of cellulose or holocellulose and by the presence of a band at 905 cm^{-1}, which is related to amorphous cellulose [32]. No bands attributable to lignin (at about 1500 and 1600 cm^{-1}) were found, a result confirmed by the phloroglucinol and Graff C tests: no red colour has been obtained by adding phloroglucinol reagent on cardboard fibres, and the result of the Graff C test was a grey/violet stain. Based on this result, it is possible to hypothesize that cardboard was obtained by chemically treated wood pulp. It should be noted that the spectra also indicate the presence of carbonates (bands at 1420 to 874 cm^{-1}), related to the alkaline reservoir of the samples, which accounts for the relative goodness of the pH values found, ranging from 5.20 $\pm$ 0.10 to 6.00 $\pm$ 0.10, as typically observed in historical cardboard materials (Table S1 in the Supplementary Materials).

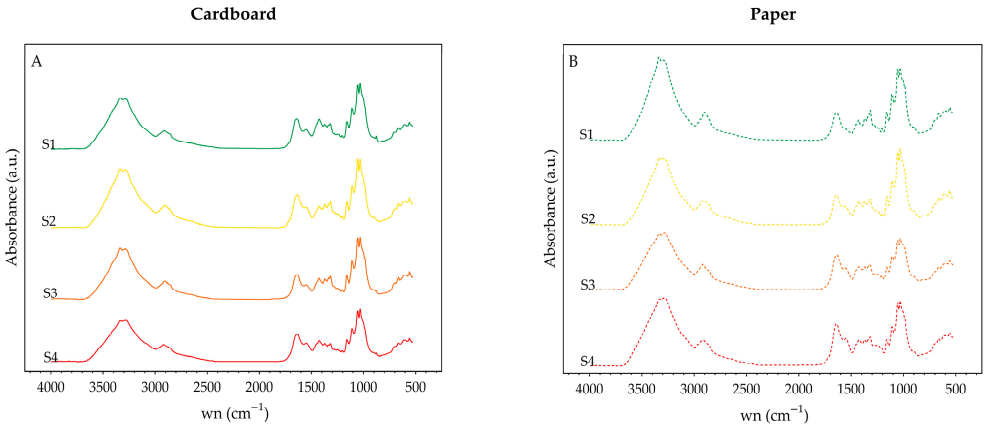

Figure 7. FTIR spectra of cardboard (**A**) and paper (**B**) fragments of the four *Compositionum* volumes. S1 to S4 refers to each of the degradation stage of the matrices.

Animal glue/sizing presence in cardboard was evidenced by the FTIR spectra (Figure 7A), as the characteristic Amide I and Amide II bands (at 1600–1700 cm^{-1} and at 1500–1600 cm^{-1}, respectively) indicates their presence [29,33,34], which was further confirmed by the Bradford assay.

Similar results were obtained in the case of the paper samples (Figure 7B): the presence of Amide I and II bands in the FTIR spectra (Figure 7) suggests the use of gelatine as waterproofing agent during the production process. The different features among the paper spectra, as regards both the envelope of bands attributable to cellulose (1200–900 cm^{-1}) and the Amide I and II, may be due to the presence of gypsum, probably used as a filler [35]. Again, a band at 905 cm^{-1} indicated the presence of amorphous zones in the cellulose component of the sample, where degradation can be triggered. The pH of the paper samples ranged from 5.36 $\pm$ 0.10 to 6.14 $\pm$ 0.10, falling within a mildly acidic interval (Table S1 in Supplementary Materials).

4. Discussion

The four volumes of *Compositionum*, preserved in the Apostolic Vatican Archive, have shown to be an interesting model of deterioration of cultural heritage. In fact, the volumes, all made in the same way and probably weatherbeaten, show different degrees of damage in their multi-material composition. Hence, in these volumes it is possible to evaluate the rate/type of degradation in each of the three matrices that make up each volume, i.e., parchment, cardboard and paper. The analyses have been performed according to a multidisciplinary approach: (i) *DNA metabarcoding* using Next Generation Sequencing to get information on the microbial colonizers (bacteria and fungi), (ii) *Raman spectroscopy* to get information on the parchment stained areas, (iii) *Light Transmission Analysis* to get information on the parchment deterioration and (iv) *FTIR spectroscopy and spot tests* to get information on the cardboard/paper deterioration. These different techniques gave several answers to different questions, allowing the reconstruction of a fairly complete picture; the results are discussed and reported according to the matrix.

4.1. Parchment

Parchment is the outer coating of the books (showing a wrapped-board semi-limp binding); hence, it has been exposed more than the other matrices to environmental biodeteriogens, which were allowed to grow because of the exposure to weather beaten. *Actinobacteriota* was the dominant bacterial phylum in the first three deterioration stages: among them the ubiquitous environmental *Pseudonocardia* and *Saccharopolyspora* genera, already reported in metagenomic studies of ancient parchment [8–10,36,37], were

abundant. In particular, *Pseudonocardia* was frequently found on aged protein-based substrates, while *Saccharopolyspora* has been commonly detected on historical parchments and proteinaceous materials [36,38], probably because of their production of resting stages (spores) [39,40] that may accumulate on the artefacts. Microorganisms belonging to these genera are known to be the last colonisers of the successional process in parchments [8,9] and can be found as dominant, due to the possible limited availability of the oldest DNA compared to the most recent environmental colonizers, quantitatively exceeding the old ones and being easily detectable due to their good DNA conservation status [10]. This dynamic can explain the result found for the first three deterioration stages: it might depend on the flattened, two-dimensional representation of the colonization process provided by the metagenomic analysis *vs*. the real three-dimensional perspective, including the accumulation of resting stages and the stratification of generations of different microbes, succeeded over centuries [10]. To further support this hypothesis, it is worth to note that in the first three deterioration stages the parchment bacterial community changed, slightly but continuously, with the increased biodeterioration: in fact, alpha diversity (Table 3) increased from stage 1 to stage 3 (H' from 3.11 $\pm$ 0.28, to 4.12 $\pm$ 0.04, to 4.41 $\pm$ 0.04), showing an increase of biodeteriogens, as typically happens along the successional processes. A completely different picture was found at stage 4, when the historical flattened perspective is overwhelmed by a very active and rich community: *Actinobacteriota* plunged and *Pseudomonadota* became dominant, with a very high alpha diversity (H' = 6.33 $\pm$ 0.04). At this stage, the already damaged (and more readily available) parchment collagen matrix allows the growth of a variety of microbes: Gram-negative bacteria *Xanthomonadales*, including both phytopathogenic genera (e.g., *Xanthomonas*) and environmental taxa (e.g., *Stenotrophomonas*) were found. Due to their notable metabolic adaptability, these bacteria are able to colonise several environments, even adverse ones, and possess enzymatic potential necessary to degrade plant polysaccharides, such as cellulose [41]. In addition, these bacteria have been already detected at low abundances in damaged parchments [42]. The functional data regarding the bacterial parchment colonizers outlines a coherent path of microbial succession. The first three stages are strongly dominated by *Actinobacteriota*, whose activities are assigned by FAPROTAX to aerobic (chemo)heterotrophy; the last stage was more diverse: the increase in *Pseudomonadota*, highlighting new functional categories, like chitinolysis (possibly related to fungal colonization, see the next paragraph), in addition to the previous aerobic (chemo)heterotrophy.

The other important player in the cultural heritage biodegradation process is the fungal community: in the same framework of the flattened, two-dimensional representation of the colonization process provided by DNA metabarcoding, parchment is consistently dominated across all four stages by ubiquitous environmental *Ascomycota*, particularly *Onygenales*, and less represented by *Eurotiales*. *Onygenales* has repeatedly been reported in biodeteriorated parchment and other protein-based historical materials [36–38], as many of them are keratinolytic and collagenolytic taxa, capable of exploiting the nitrogen-rich protein matrix of parchment and making them primary agents of its degradation [43]. Among the *Eurotiales*, the genera *Penicillium* and *Aspergillus* were commonly found. It is interesting to underline that, at increased biodeterioration, other taxa were recruited: at stage 4, minor occurrences of the *Microascales* and *Sordariales* orders were detected; among them the *Microascaceae* and *Chaetomiaceae* families, common indoor or archival environment colonizers, typically associated with the deterioration of plant-based matrices, as they produce cellulolytic enzymes [44,45]. Their association with parchment is intimate, as the *Chaetomiaceae*, *Chaetomium globosum*, has been found on parchments with fruiting structures embedded in the parchment matrix [46]. *Basidiomycota* were found at very low percentages (<2%, stage 1 and stage 4; 4.05% and 4.35%, stages 2 and 3, respectively), in

particular the order *Polyporales* and *Hymenochaetales* (≃2%, stages 2 and 3). Some of them are efficient degraders of lignin and other highly recalcitrant structural polymers, according to their role of *late-stage degraders* in terrestrial systems [47]. Their presence in parchment, although limited, may reflect their ability to colonize collagen matrices already weakened or significantly altered.

The fungal colonizers are known to be typical of the final phases of the successional process: in fact, their alpha diversity is low at stage 1 (H' = 2.46 ± 0.16) but abruptly increased at stage 2 remaining quite constant as the degradation process progresses (from stage 2 to 4, ranging from 4.53 ± 0.43 to 4.15 ± 0.93 to 4.57 ± 0.39), without statistically significant differences. Functional data on parchment fungal colonizers also outline a consistent biodegradation pathway. FUNGuild analysis, which focus on the putative trophic or metabolic function of fungal taxa, confirmed the dominance of saprotrophic or pathotrophic–saprotrophic guilds, compatible with the presence of organisms capable of exploiting both native collagen and its degradation products. For instance, the dominant *Onygenales* account for keratinolytic and collagenolytic taxa, which may act as degraders of the protein matrix.

A final consideration must be dedicated to the overall dominance of *Actinobacteria* (like *Saccharopolyspora*) and *Ascomycetes* (*Penicillium* and *Aspergillus*, among others); it may again be related not only to their DNA abundance, but also to the presence of apparently integer cells and spores [36,46] and their ability to endure unfavourable environmental conditions.

The effect of microbial colonization on the parchment matrix has been measured by Light Transmission Analysis (LTA), allowing for the evaluation of the denaturation temperature of the collagen, which is correlated with the hydrothermal stability of the samples: the higher the denaturation temperature, the better will be the chemical integrity of the collagen fibres, and, therefore, the preservation of the sample [24]. In unstained areas, the denaturation temperature of the native collagen progressively decreased from stage 1 (56.07 °C) to stage 4 (46.27 °C), indicating an increased collagen deterioration across the stages: at stage 1, the least damaged, the collagen fractions are present and well preserved in the matrix, showing the highest T_d; then, from stage 1 to 4, a steady T_d decrease was observed, with statistically significant differences. Conversely, in stained areas, T_d decreased from stage 1 to stage 3 (from 55.77 to 48.27 °C), as in the unstained areas, but showed a slight increase at stage 4, rising to 50.30 °C. This non-monotonic behaviour might be due to the heterogeneity of the parchment and of the degradation rate; however, an alternative hypothesis is that it may depend on the presence of one of the microbial colonizers, the fungi, which grow within the collagen matrix producing an intertwined three-dimensional hyphal network that could stabilize the matrix despite its structural depletion. More extensive sampling and measurements could confirm the causal agent; however, this has been impossible for the *Compositionum* volumes, due to the limited availability of samples.

Raman spectroscopy provided complementary chemical evidence for the interpretation of the dark discolouration observed on the damaged areas of the parchment. Specifically, the spectra showed characteristics comparable to those reported for melanin [30,31] and all stages produced coloured extracts, consistent with the presence of this pigment. In particular, the stage 2 sample showed the most intense coloration, and a melanin residue has been isolated. The fungal taxa *Capnodiales* produces DOPA-type melanin (L-3,4-dihydroxyphenylalanine) [48] and is frequently associated with the formation of dark spots on documents [37,49,50]. However, *Capnodiales* were detected on parchment at low relative abundance; however, this low abundance melanising taxa could be attributed to these taxa being underrepresented in metabarcoding datasets. Furthermore, both the persistence of melanin and its ability to remain associated with biological substrates has

been demonstrated [51]. The progressive structural weakening of the matrix could promote secondary chemical pathways leading to the formation or stabilization of melanin-like compounds [52]. The high microbial activity responsible of the matrix alteration could create favourable conditions for melanin accumulation.

Overall, Raman and UV–Vis spectroscopy confirm the presence of melanin and its role in parchment discolouration. Melanin, therefore, should be considered in the study of ancient documents, being a good marker, with significant implications in the stain comprehension and conservation strategies.

In conclusion, all these results clearly agree with the previous studies about the parchment deterioration [8–10,46]. Although the initial dominance of ubiquitous bacterial and fungal taxa (*Pseudonocardiales* and *Onygenales*, respectively), the subsequent occurrence of additional bacterial phyla (*Pseudomonadota*) and new fungal orders (*Eurotiales*, *Microascales*, *Sordariales*), determining the increase in both bacterial and fungal alpha diversity, indicated the progression of the microbial succession. This dynamic is consistent with the model proposed by Migliore et al. [8,9] for the parchment purple spot deterioration, indicating that the four *Compositionum* book parchment covers represents different phases of a heterotrophic succession [10]. Inside this process, the heavily biodeteriorated parchment matrix showed unclear dynamics, with a possible explanation being in the fungal colonization 'deceptively' mimicking the structured matrix with its intertwined hyphal network.

4.2. Cardboard

In wrapped-board, semi-limp binding cardboard constitutes the stiffening materials beneath the covering parchment of the books. Although less exposed to biodeteriogens than the parchment, the cardboard showed a diverse biodeteriogens community at all stages of deterioration, with the presence of several environmental and cellulose-associated taxa, due to its peculiar composition and structure. In fact, cardboard is a heterogeneous matrix processed using animal and plant glues, representing a variety of substrates suitable for different microbial taxa. In addition to the plant-based components, FTIR analysis confirmed the presence of animal glue in the cardboard, highlighting the characteristic bands of Amides I and II [53]. These protein substrates promote microbial colonization: for instance, the genera *Aspergillus* and *Penicillium*, capable of degrading both cellulose fibres and animal-based adhesives, contribute to the deterioration of the matrix [37,54]. Similarly, bacteria belonging to the *Bacillales* order, thanks to their production of proteases and collagenases, can exploit animal glue as a source of nutrients, collaborating with fungi in the cardboard biodeterioration [4,55]. Furthermore, its porous structure retains water more effectively than parchment, generating microenvironments that support microbial adhesion and community diversification. These physical and chemical characteristics, combined with the fluctuating humidity and limited air circulation, typical of archival preservation [56], make it particularly susceptible to colonization by environmental bacteria capable of tolerating humidity fluctuations and periods of nutrient scarcity [57]. The order *Bacillales* (belonging to the phylum *Bacillota*) was the dominant bacterial order in all four deterioration stages, probably depending on its capability to produce spores that persist for long time periods and can be reactivated as microclimatic conditions turn favourable, as in the presence of water or high relative humidity [4,58]. Members of this order are known for their metabolic versatility and capability to produce a wide range of hydrolytic enzymes, including proteases, collagenases, cellulases, and amylases, which allow them to exploit both animal-derived glues and cellulose fibres [37,55]. Thanks to this broad-spectrum enzymatic activity, *Bacillales* play a crucial role in the biodeterioration of cardboard, in addition to the observed activity on parchment. In all stages, the orders *Clostridiales* and *Pseudonocardiales* were also detected, albeit in percentages lower than 20%. *Clostridiales*

are cellulolytic bacteria and are commonly associated to the deterioration processes and with the decay of organic matter [59]; their spores are highly resistant and can reactivate in the presence of water and high humidity levels [4]. *Pseudonocardiales* are known for their ability to degrade cellulose above all but are also capable of degrading protein substrates. Indeed, their greater abundance on parchment, as previously mentioned, could be due to the fact that it constitutes the book cover, which is therefore more exposed than the cardboard under jacket. Their detection accounts for the most available environmental colonizers, favoured by the porous structure and mixed composition of the cardboard [57]. The bacterial community remained stable across the first stages: alpha diversity values (Figure 3) are quite high from stage 1 to 3 (H' from 7.49 ± 0.06 to 7.60 ± 0.07 to 7.40 ± 0.39) and slightly decreased at stage 4 (H' = 6.33 ± 0.09), probably due to the reduction of nutrients. FAPROTAX analysis highlighted that the main functional role of the bacterial community in cardboard is chemoheterotrophy, which is associated with the use of cellulosic substrates, depending on the presence of several environmental taxa (*Bacillales* and *Pseudonocardiales*). Across all deterioration stages, chemoheterotrophy (representing 41% to 50% of the community) and aerobic chemoheterotrophy (representing 30–45%) are the most represented functional activity, suggesting that cardboard degradation is mainly driven by metabolically versatile aerobic bacteria. Cellulolytic and chitinolytic activities are less abundant and present only in stage 1 (3%) and stage 4 (2%); however, they are relevant in explaining the degradation processes of cellulosic material.

The fungal community of cardboard is characterized by the presence of *Eurotiales* in all four stages, unlike what was found on parchment (dominant *Onygenales*). *Eurotiales* are a ubiquitous order of filamentous fungi characteristic of microenvironments with fluctuating humidity and poor ventilation, which are typical conditions found in archives and warehouses [11,49,54]. Their dominance can be explained by the presence of spores that are highly resistant to humidity fluctuations [4,49]. In particular, the genus *Aspergillus* is dominant in all four stages, representing 98% of the *Eurotiales*. This genus, along with *Penicillium* and *Eurotium*, are known to produce enzymes such as cellulases, hemicellulases, and amylases able to degrade cellulose fibres and starch-based adhesives commonly found in cardboard [11,37,54]. These taxa are also capable of producing organic acids, pigments and volatile metabolites that may cause surface discoloration, pH changes and fibre weakening, acting as both biochemical and mechanical agents of biodeterioration [4,60,61]. Hence, the damage observed on these volumes, including brownish stains, fibre weakening (holes and rips) and page compaction, can be attributed to the fungal thriving and activity [11,60,62]. Moreover, it is probably the combined action of fungi and bacteria, which possess effective and diverse enzymatic systems, that contributes to the structural weakening of the cellulose fibres [4,14]. Minor presences of *Onygenales* were detected at all stages. These fungi are generally considered opportunistic colonizers of late seral successional stages, rather than pioneer biodeteriogens, and grow by exploiting denatured organic matter and byproducts released by *Eurotiales* [37,38,43]. Their behaviour shows an opposite trend compared to that found in parchment, where *Onygenales* dominate all stages as pioneer degraders of the protein matrix. In cardboard, their low abundance likely reflects the scarcity of keratinous or collagenous substrates, which limits their success on cellulose-based materials. As found in bacteria, fungal alpha diversity also increased during the first phases of the deterioration process, peaking at stage 3 (H' from stage 1, 3.27 ± 0.87; stage 2, 6.36 ± 0.23; stage 3, 7.06 ± 0.26), and declined at stage 4 (H' = 5.37 ± 0.95), again probably related to the reduction of nutrients. However, this suggests that deterioration affects the relative abundance of minor taxa, while the overall community structure remains stable. This pattern is consistent with general models of heterotrophic fungal succession, in which community structure remains relatively stable over time, while turnover among minor

taxa is observed in response to resource quality and microenvironmental changes [63]. The FUNGuild analysis highlighted the dominance of saprotrophic guilds (representing 21–51% of the community), depending on the presence of *Eurotiales*: the cellulolytic and amylolytic enzymes of *Aspergillus* are responsible for fibres weakening and stains on the matrix. Mixed groups, such as the pathotroph–saprotroph one, are stable across all stages and depend on the presence of *Onygenales*. In addition, this pathotroph–saprotroph group can also be related to the presence of opportunistic taxa that are capable of exploiting already degraded substrates and surviving in fluctuating environmental conditions. The pathotroph–saprotroph–symbiotroph group showed an increase at stage 4, suggesting greater functional complexity and interaction between taxa in the more advanced stages of degradation.

Overall, the integration of taxonomic and functional data shows that cardboard, thanks to its porous nature, moisture-retaining capacity and mixed composition of cellulose fibres and animal/plant glues, represents a highly favourable matrix for microbial colonization [4,64]. Unlike parchment, cardboard hosts heterogeneous microbial communities, dominated by environmental and metabolically versatile groups. The dominance of *Bacillales* and *Eurotiales*, combined with increased alpha diversity in the intermediate stages of degradation, suggests that colonization of this type of matrix is primarily driven by aerobic bacteria and fungi that degrade organic-based cellulosic substrates. The identified functions (chemoheterotrophy in bacteria, saprotrophy and pathotrophy in fungi) highlight an ongoing degradative activity, which contributes to the fibres weakening and the discolouration of the matrix.

Hence, in cardboard, microbial succession is driven by the substrate, selecting bacterial and fungal strains capable of degrading cellulose and animal/plant glues. Bacterial communities remain stable in the initial stages, while fungal communities' peaks in the intermediate stages, probably depending on the availability of new breakdown products of cellulose degradation that gradually become available and on the matrix-specific degradation dynamics.

4.3. Paper

Paper, which constitutes the internal book block, represents the less exposed matrix to environmental biodeteriogens; nevertheless, under permissive conditions (i.e., high relative humidity), its cellulose-based composition provides a suitable substrate for microorganisms capable of hydrolysing polysaccharides and starch adhesives. As observed for cardboard, the paper matrix also showed microbial colonization and enzymatic degradation of cellulose and adhesives. Furthermore, in paper the presence of animal-based glues was also confirmed by FTIR analysis.

In the four *Compositionum* book blocks we found a microbial community ruled by the degree of deterioration: *Pseudonocardiales* and *Bacillales* were the dominant orders across the first three stages, as they are environmental bacteria with a well-known enzymatic array able to degrade cellulose and starch-based compounds [57,60]. Differently, a marked increase in *Sphingobacteriales* (66.84%) was observed in stage 4: some species of this order are able to degrade complex organic polymers—such as cellulose, hemicellulose and pectin—and are often found in late colonisation stages of heterotrophic succession [65]. Their abundance suggests a shift toward a functionally adapted community able to thrive in nutrient-enriched/diversified environments [66], as in the most degraded stage an accumulation of breakdown products may occur. Alpha diversity values confirmed the shift toward a functionally adapted community: a significant variation along the deterioration process was found (Figure 3; $p < 0.05$), with the highest values observed in the intermediate phases ($H' = 8.15 \pm 0.25$ and 7.92 ± 0.04 at stages 2 and 3, respectively) and low values

at the beginning and at the end of the process (H′ = 5.70 ± 0.76 and 5.31 ± 0.15 at stages 1 and 4, respectively). This pattern suggests that the bacterial community becomes more diversified during the intermediate phases of deterioration (stages 2 and 3), as a response to increased/diversified resource availability, whereas advanced degradation and reduction of nutrients lead to a shift towards few specialized bacterial taxa. Consistent with this dynamic, FAPROTAX analysis showed a functional change along the deterioration process: aerobic heterotrophy and chemoheterotrophy were dominant in all stages (relative abundance from 32 to 41% in stages 2 and 4, and from 39 to 48%, in stages 1 and 3, respectively), when *Pseudonocardiales*, *Bacillales*, and *Sphingobacteriales* occurred. Fermentation was only present in the initial stages, then progressively decreased (11% stage 1, 4% stage 2 and 5% stage 3) and completely disappeared in stage 4, indicating that this process probably acts when the cellulose structure is still present or minimally degraded [67]. More specialized functions, such as methylotrophy and methanol oxidation, appeared exclusively in stage 2 (2%), while chitinolysis appears only in stage 4 (2%), probably due to the widespread presence of fungi on/in the matrix, which provide the chitinous substrate (derived from fungal cell walls) useful for bacteria able to degrade chitin, as with *Bacillus* and *Brevibacterium* (*Bacillales* and *Micrococcales* orders, respectively). This supports the hypothesis that in the more advanced stages bacteria capable of degrading polymers and complex residues are recruited.

The fungal community of the paper showed limited taxonomic variations along the degradation process, although displaying the pattern of a successional process. In all stages, *Eurotiales* were the dominant order, particularly in stage 3 (50%), and the abundance of *Aspergillus* sp. confirms the adaptation of xerophilic and cellulolytic fungi to the paper microenvironment, as observed in previous studies on archival materials [11,49,54]. In addition, *Capnodiales*, were detected across all stages with a relative abundance of 21% in stage 1, 12% in stage 2, 10% in stage 3 and 16% in stage 4. *Capnodiales* are known to produce melanin and other dark pigments that contribute to surface discolouration and visual staining of the paper supports [37,50,60]. *Polyporales* are present in all four stages, with a relative abundance of 18% in stages 1 and 4, 13% in stage 2 and 10% in stage 3. They are known to be efficient degraders of lignin and other highly recalcitrant structural polymers. *Onygenales* are nearly absent from the paper matrix, although present in cardboard and dominant on parchment, reflecting the decreasing gradient of proteinaceous compounds from the outer to the inner section of the book. This pattern indicates that fungal colonization is strongly influenced by substrate composition, with *Onygenales* occurring where nitrogen-rich materials are available, while *Eurotiales* prevail in carbohydrate-dominated environments [4,37,43]. Fungal alpha diversity is quite high in the initial and final stages of deterioration (H′ = 7.32 ± 0.79 and 7.29 ± 0.40 in stages 1 and 4, respectively), highlighting that a wide range of colonizers dominate the early stages, whereas in the late stages specialized decomposers become prevalent, according to the resources available in the damaged matrix. This is the opposite trend to that found in bacterial communities, where diversity decreases in the final phase (H′ = 5.31 ± 0.15). This probably depends on the available substrates in the final degradation phase when the residual complex polymers select the specialized taxa able to degrade them. FUNGuild analysis showed that saprotrophy dominates in all stages, with values ranging from 41% to 61%, due to the primary role of fungi in cellulose degradation. Pathotroph–saprotrophs haphazardly changed along the degradation process (29%, 27%, 39% and 23%, from stage 1 to 4), mainly represented by *Capnodiales*, present in all four degradation stages. Instead, pathotroph–saprotroph–symbiotrophs, mainly represented by *Eurotiales*, increased in the last two stages (6%, 5%, 17% and 18%, from stage 1 to 4), probably reflecting the progressive availability of new resources derived from the cellulose degradation and metabolic by-products.

Overall, the paper matrix shows a deterioration path consistent with its structural characteristics, although bacterial and fungal communities respond differently to the progressive degradation. Bacterial communities showed a low diversity in the initial and last stages and a high diversity in the intermediate stages, as previously reported: this trend is consistent with the presence of a heterotrophic succession. The matrix is still intact in stage 1, providing limited resources to few taxa such as *Pseudonocardiales*, that can exploit cellulose and starch. In stages 2 and 3, the degradation progresses and the breakdown of cellulose and polysaccharides produces abundant resources, supporting a diversified bacterial community. In the final part of the degradation process (stage 4), the substrate becomes selective and limited for bacteria, favouring specialized taxa such as *Sphingobacteriales*. Conversely, fungal communities showed a high diversity in the initial and last stage and a reduced diversity in the intermediate stages. At stage 1, the intact matrix provides readily accessible resources, allowing the coexistence of many fungal colonizers, including *Capnodiales*, responsible for the surface discoloration. In stages 2 and 3, the substrate becomes increasingly selective, and only specialized cellulolytic fungi, such as *Eurotiales*, can efficiently exploit the remaining cellulose. By stage 4, the matrix is largely degraded and organic residues generated by previous bacterial and fungal activities provide additional accessible resources, allowing a broad range of fungal taxa to coexist. In the end, the degradation community behave and integrate differently: bacteria respond primarily to chemical heterogeneity of the substrate, whereas fungi respond to both resource availability and matrix structural or spatial features [68]. As found in paperboard, the microbial succession in paper matrix is driven by substrate composition, as the found bacteria and fungi degrade cellulose and adhesives through their enzymatic activities. Bacterial communities showed the highest diversity in the intermediate stages, primarily responding to substrate composition. In contrast, fungal communities, with the highest diversity in the early and late stages, have been shown to respond to both resource availability and substrate composition. Overall, these dynamics reflect specific matrix degradation within a framework of heterotrophic succession models.

To conclude, the main actors of the biodegradation process and the degradation dynamics in the different matrices were identified. The results demonstrated that the dynamics of the microbial succession in ancient books/archival documents are influenced by the characteristics of each matrix and future studies on whole multi-material artifacts must take into consideration all different matrices and their dynamics.

Furthermore, to answer the last questions to which this study was dedicated, i.e., the possible transfer of biodeteriogens between matrices due to their physical proximity, beta diversity offered initial but robust evidence. The analyses demonstrated a clear separation between the parchment and the other two cellulose-based matrices, and a different pattern for bacteria and fungi. As regards bacteria, all matrices are colonized by different communities. The parchment community remains distinct at the taxonomic and functional level, as taxa such as *Xanthomonadales*, can be found in parchment but are absent/rare in cardboard and paper. Their confinement to parchment reflects their ability to colonize the collagen in the cover without significant transfer to the inner cellulosic matrices, lacking/poor in nutrients of animal origin. Neither cardboard nor paper bacterial community profiles overlap, notwithstanding their similar composition. The differences reflect the structural specificity of the two cellulose-based matrices: cardboard, with its porous structure and the presence of animal and/or plant glues, hosts metabolically versatile environmental groups, such as *Bacillales* and *Clostridiales*, whereas paper is dominated by *Pseudonocardiales* and *Sphingobacteriales*, showing a marked increase at the last stage, a pattern presumably linked to the advanced cellulose degradation. As regards fungi, the pattern is different. In parchment a well-defined and clearly separated cluster can be found consistent with its

proteinaceous composition and with the dominance of specialized taxa such as *Onygenales*, due to their keratinolytic and collagenolytic activity. Conversely, although significantly different, in cardboard and paper a partial fungal community overlap can be found, reflecting their shared capability to thrive on cellulose-based matrices. Despite this overlap, the two matrices maintain recognizable differences: cardboard exhibits a similar fungal profile across the degradation process, probably linked to their structure (thick and porous), while paper hosts a variable community across the stages presumably recruited by breakdown products availability, resulting by the bacterial activity of taxa such as *Pseudonocardiales* and *Sphingobacteriales*, which are able to degrade cellulose and starch-based compounds. Furthermore, both bacterial and fungal communities showed a progressively increased diversity from parchment to cardboard to paper, probably depending on the homogeneity and biodegradability of the matrices: for instance, paper can host several taxa depending on the several breakdown products of cellulose, hemicellulose, etc., produced by both bacterial and fungal biodegradative activities.

To conclude, the *Compositionum* books gave no evidence of significant microbial transfer across the three matrices, and microbial patterns reflected substrate affinity rather than cross-matrix transfer. As final consideration, this study highlights the importance of integrating biological, chemical and physical data in order to better understand the biodeterioration processes affecting ancient library artefacts. The matrix-specific analyses performed here show that parchment, cardboard and paper each display distinct microbial successions and degradation pathways, without significant cross-contamination, underscoring the need to investigate every substrate independently. Indeed, given that these materials coexist within a single multi-material object, assessing whether they might interact or influence one-another is essential for developing conservation strategies. Even when no cross-matrix transfer is detected, shared environmental conditions and the physical juxtaposition of the materials can shape the overall deterioration pattern. The techniques used in this study, together with the results obtained, clarified which microbial groups recur in association with each matrix and deterioration stage in the *Compositionum* volumes. Scientific analysis, therefore, represents an important link with conservation and restoration practices, offering evidence that can support both preventive monitoring and the planning of appropriate preservation strategies.

Supplementary Materials: The following supporting information can be downloaded at: https://www.mdpi.com/article/10.3390/app16021091/s1, Figures S1–S8: LTA denaturation curves comparing unstained and stained areas in the parchment matrix across all the four deterioration stages (from 1 to 4). Peak 1: TN, native collagen population; Peak 2: Ts, stabilized collagen population. A and B: parchment stage 1. C and D: parchment stage 2. E and F: parchment stage 3. G and H: parchment stage 4; Figure S9: Typical Raman spectrum at 532 nm of untreated samples with a strong photoluminescence background; Table S1: pH surface values of the cardboard and paper samples. Table S2: OTUs taxonomic identification of (A) bacteria and (B) fungi.

Author Contributions: Conceptualization, L.M., C.G. and A.R.; methodology, C.G., A.A., M.M.D., S.F., V.G., C.M., N.O., B.E. and S.P.; formal analysis, C.G., A.A., M.M.D., N.O. and L.M.; resources, L.M., C.M. and A.R.; writing—original draft preparation, C.G., A.A., C.M. and L.M.; and writing—review and editing, C.G., A.A., M.M.D., S.F., V.G., C.M., N.O., S.P., A.R. and L.M. All authors have read and agreed to the published version of the manuscript.

Funding: C.G. has a three-year PNRR DM118 Ph.D. scholarship funded from the Ph.D. Program in Evolutionary Biology and Ecology, University of Rome Tor Vergata, in collaboration with the Apostolic Vatican Archives (Vatican City).

Institutional Review Board Statement: Not applicable.

Informed Consent Statement: Not applicable.

Data Availability Statement: The raw data generated for the 16S and ITS2-5.8S amplicon projects have been deposited at the NCBI Sequence Read Archive (SRA) under BioProject ID PRJNA1381600.

Acknowledgments: The authors are indebted to Rev.mo Father Rocco Ronzani, *Ordo Sancti Augustini*, who gave us the unique opportunity to work in the incredible context of the Apostolic Vatican Archives, among its kilometres of shelving and thousands of documents. The authors CM, VG and BE wished to thank the MUR Grant for Dipartimento di Eccellenza 2023-27 X-CHEM project "eXpanding CHEMistry: implementing excellence in research and teaching". The authors are grateful to Fulvio Mercuri, Silvia Orlanducci and Ugo Zammit for their advice in all phases of the work; without them we would not have achieved the level of insight we got. Last but not least, the authors are in debt with Cristina Cicero for her precious suggestions on the ancient book world and nomenclature.

Conflicts of Interest: The authors declare no conflicts of interest. The funders had no role in the design of the study; in the collection, analyses, or interpretation of data; in the writing of the manuscript; or in the decision to publish the results.

References

1. Welker, F. Palaeoproteomics for Human Evolution Studies. *Quat. Sci. Rev.* **2018**, *190*, 137–147. [CrossRef]
2. Buckley, M. Paleoproteomics: An Introduction to the Analysis of Ancient Proteins by Soft Ionisation Mass Spectrometry. In *Paleogenomics: Population Genomics*; Lindqvist, C., Rajora, O., Eds.; Springer: Cham, Switzerland, 2018; pp. 31–52.
3. Bajpai, P. Brief Description of the Pulp and Papermaking Process. In *Biotechnology for Pulp and Paper Processing*; Springer: Singapore, 2018; pp. 9–26.
4. Joseph, E. *Microorganisms in the Deterioration and Preservation of Cultural Heritage*; Springer Nature: Cham, Switzerland, 2021.
5. Hueck, H.J. The Biodeterioration of Materials—An Appraisal. In *Biodeterioration of Materials*; Walters, A.H., Elphick, J.J., Eds.; Elsevier: Amsterdam, The Netherlands, 1968; pp. 6–12.
6. Branysova, T.; Demnerova, K.; Durovic, M.; Stiborova, H. Microbial Biodeterioration of Cultural Heritage and Identification of the Active Agents over the Last Two Decades. *J. Cult. Herit.* **2022**, *55*, 245–260. [CrossRef]
7. Odum, E.P. *Fundamentals of Ecology*; Saunders: Philadelphia, PA, USA, 1953.
8. Migliore, L.; Thaller, M.C.; Vendittozzi, G.; Mejia, A.Y.; Mercuri, F.; Orlanducci, S.; Rubechini, A. Purple Spot Damage Dynamics Investigated by an Integrated Approach on a 1244 A.D. Parchment Roll from the Secret Vatican Archive. *Sci. Rep.* **2017**, *7*, 9521. [CrossRef] [PubMed]
9. Migliore, L.; Perini, N.; Mercuri, F.; Orlanducci, S.; Rubechini, A.; Thaller, M.C. Three Ancient Documents Solve the Jigsaw of the Parchment Purple Spot Deterioration and Validate the Microbial Succession Model. *Sci. Rep.* **2019**, *9*, 1623. [CrossRef] [PubMed]
10. Perini, N.; Mercuri, F.; Orlanducci, S.; Thaller, M.C.; Migliore, L. The Integration of Metagenomics and Chemical Physical Techniques Biodecoded the Buried Traces of the Biodeteriogens of Parchment Purple Spots. *Front. Microbiol.* **2020**, *11*, 598945. [CrossRef] [PubMed]
11. Abdel-Maksoud, G.; Abdel-Nasser, M.; Sultan, M.H.; Eid, A.M.; Alotaibi, S.H.; Hassan, S.E.-D.; Fouda, A. Fungal Biodeterioration of a Historical Manuscript Dating Back to the 14th Century: An Insight into Various Fungal Strains and Their Enzymatic Activities. *Life* **2022**, *12*, 1821. [CrossRef]
12. Karakasidou, K.; Nikolouli, K.; Amoutzias, G.D.; Pournou, A.; Manassis, C.; Tsiamis, G.; Mossialos, D. Microbial Diversity in Biodeteriorated Greek Historical Documents Dating Back to the 19th and 20th Century: A Case Study. *MicrobiologyOpen* **2018**, *7*, e00596. [CrossRef]
13. Manente, S.; Micheluz, A.; Ganzerla, R.; Ravagnan, G.; Gambaro, A. Chemical and Biological Characterization of Paper: A Case Study Using a Proposed Methodological Approach. *Int. Biodeterior. Biodegrad.* **2012**, *74*, 99–108. [CrossRef]
14. Stratigaki, M.; Armirotti, A.; Ottonello, G.; Manente, S.; Traviglia, A. Fungal and Bacterial Species Richness in Biodeteriorated Seventeenth Century Venetian Manuscripts. *Sci. Rep.* **2024**, *14*, 7003. [CrossRef]
15. Takahashi, S.; Tomita, J.; Nishioka, K.; Hisada, T.; Nishijima, M. Development of a Prokaryotic Universal Primer for Simultaneous Analysis of Bacteria and Archaea Using Next-Generation Sequencing. *PLoS ONE* **2014**, *9*, e105592. [CrossRef]
16. White, T.J.; Bruns, T.; Lee, S.W.T.; Taylor, J. Amplification and direct sequencing of fungal ribosomal RNA genes for phylogenetics. In *PCR Protocols: A Guide to Methods and Applications*; Academic Press, Inc.: Cambridge, MA, USA, 1990; Volume 18, pp. 315–322.
17. Tedersoo, L.; Bahram, M.; P.lme, S.; K.ljalg, U.; Yorou, N.S.; Wijesundera, R.; Abarenkov, K. Global diversity and geography of soil fungi. *Science* **2014**, *346*, 1256688. [CrossRef]
18. Bolyen, E.; Rideout, J.R.; Dillon, M.R.; Bokulich, N.A.; Abnet, C.C.; Al-Ghalith, G.A.; Caporaso, J.G. Reproducible, interactive, scalable and extensible microbiome data science using QIIME 2. *Nat. Biotechnol.* **2019**, *37*, 852–857. [CrossRef]

19. Callahan, B.J.; McMurdie, P.J.; Rosen, M.J.; Han, A.W.; Johnson, A.J.A.; Holmes, S.P. DADA2: High-resolution sample inference from Illumina amplicon data. *Nat. Methods* **2016**, *13*, 581–583. [CrossRef]
20. Quast, C.; Pruesse, E.; Yilmaz, P.; Gerken, J.; Schweer, T.; Yarza, P.; Peplies, J.; Glöckner, F.O. The SILVA ribosomal RNA gene database project: Improved data processing and web-based tools. *Nucleic Acids Res.* **2012**, *41*, D590–D596. [CrossRef]
21. Kõljalg, U.; Nilsson, R.H.; Abarenkov, K.; Tedersoo, L.; Taylor, A.F.S.; Bahram, M. Towards a unified paradigm for sequence-based identification of fungi. *Mol. Ecol.* **2013**, *22*, 5271–5277. [CrossRef]
22. Louca, S.; Parfrey, L.W.; Doebeli, M. Decoupling Function and Taxonomy in the Global Ocean Microbiome. *Science* **2016**, *353*, 1272–1277. [CrossRef] [PubMed]
23. Nguyen, N.H.; Song, Z.; Bates, S.T.; Branco, S.; Tedersoo, L.; Menke, J.; Schilling, J.S.; Kennedy, P.G. FUNGuild: An Open Annotation Tool for Parsing Fungal Community Datasets by Ecological Guild. *Fungal Ecol.* **2016**, *20*, 241–248. [CrossRef]
24. Cicero, C.; Mercuri, F.; Paoloni, S.; Orazi, N.; Zammit, U.; Glorieux, C.; Thoen, J. Integrated Adiabatic Scanning Calorimetry, Light Transmission and Imaging Analysis of Collagen Deterioration in Parchment. *Thermochim. Acta* **2019**, *676*, 263–270. [CrossRef]
25. Badea, E.; Della Gatta, G.; Usacheva, T. Effects of Temperature and Relative Humidity on Fibrillar Collagen in Parchment: A Micro Differential Scanning Calorimetry (Micro DSC) Study. *Polym. Degrad. Stab.* **2012**, *97*, 346–353. [CrossRef]
26. Oh, J.J.; Kim, J.Y.; Kwon, S.L.; Hwang, D.H.; Choi, Y.E.; Kim, G.H. Production and characterization of melanin pigments derived from *Amorphotheca resinae*. *J. Microbiol.* **2020**, *58*, 648–656. [CrossRef]
27. Adamopoulos, S.; Oliver, J. Fiber composition of packaging of grade papers as deter-mined by the Graff "C" staining test. *Wood Fiber Sci.* **2006**, *38*, 567–575.
28. Davidson, R.S.; Choudhury, H.; Origgi, S.; Castellan, A.; Trichet, V.; Capretti, G. The reaction of phloroglucinol in the presence of acid with lignin-containing materials. *J. Photochem. Photobiol. A Chem.* **1995**, *91*, 87–93. [CrossRef]
29. Petrella, G.; Mazzuca, C.; Micheli, L.; Cervelli, E.; De Fazio, D.; Iannuccelli, S.; Sotgiu, S.; Palleschi, G.; Palleschi, A. A new sustainable and innovative work for paper artworks cleaning process: Gellan hydrogel combined with hydrolytic enzymes. *Int. J. Conserv. Sci.* **2016**, *7*, 273–280.
30. Capozzi, V.; Perna, G.; Gallone, A.; Biagi, P.F.; Carmone, P.; Fratello, A.; Guida, G.; Zanna, P.; Cicero, R. Raman and optical spectroscopy of eumelanin films. *J. Mol. Struct.* **2005**, *744–747*, 717–721. [CrossRef]
31. Melo, D.; Paiva, T.G.; Lopes, J.A.; Corvo, M.C.; Sequeira, S.O. Characterization of fungal melanins from black stains on paper artefacts. *Heritage* **2022**, *5*, 3049–3065. [CrossRef]
32. Zotti, M.; Ferroni, A.; Calvini, P. Microfungal biodeterioration of historic paper: Preliminary FTIR and microbiological analyses. *Int. Biodeterior. Biodegrad.* **2008**, *62*, 186–194. [CrossRef]
33. Krimm, S.; Bandekar, J. Vibrational spectroscopy and conformation of peptides, polypeptides, and proteins. *Adv. Protein Chem.* **1986**, *38*, 181–364. [CrossRef] [PubMed]
34. Maekawa, H.; Ballano, G.; Toniolo, C.; Ge, N.H. Linear and two-dimensional infrared spectroscopic study of the amide I and II modes in fully extended peptide chains. *J. Phys. Chem. B* **2011**, *115*, 5168–5182. [CrossRef] [PubMed]
35. Librando, V.; Minniti, Z.; Lorusso, S. Ancient and modern paper characterization by FTIR and Micro-Raman spectroscopy. *Conserv. Sci. Cult. Herit.* **2011**, *11*, 249–268. [CrossRef]
36. Piñar, G.; Tafer, H.; Schreiner, M.; Miklas, H.; Sterflinger, K. Decoding the Biological Information Contained in Two Ancient Slavonic Parchment Codices: An Added Historical Value. *Environ. Microbiol.* **2020**, *22*, 3218–3233. [CrossRef]
37. Sterflinger, K.; Piñar, G. Microbial Deterioration of Cultural Heritage and Works of Art-Tilting at Windmills? *Appl. Microbiol. Biotechnol.* **2013**, *97*, 9637–9646. [CrossRef]
38. Pinheiro, C.; Miller, A.Z.; Vaz, P.; Caldeira, A.T.; Casanova, C. Underneath the Purple Stain. *Heritage* **2022**, *5*, 4100–4113. [CrossRef]
39. Sayed, A.M.; Abdel-Wahab, N.M.; Hassan, H.M.; Abdelmohsen, U.R. *Saccharopolyspora*: An underexplored source for bioactive natural products. *J. Appl. Microbiol.* **2020**, *128*, 314–329. [CrossRef]
40. Riahi, H.S.; Heidarieh, P.; Fatahi-Bafghi, M. Genus *Pseudonocardia*: What we know about its biological properties, abilities and current application in biotechnology. *J. Applied Microbiol.* **2022**, *132*, 890–906. [CrossRef]
41. Ghosh, R.; Chatterjee, S.; Mandal, N.C. Stenotrophomonas. In *Beneficial Microbes in Agro-Ecology*; Elsevier: Amsterdam, The Netherlands, 2020; pp. 427–442. [CrossRef]
42. Migliore, L.; Vendittozzi, G.; Mejia, A.Y.; Mercuri, F.; Carbonetti, C.; Thaller, M.C.; Romani, M.; Cicero, C.; Orazi, N.; Pasqualucci, A.; et al. Arm. I–XVIII 3328 Dell'Archivum Arcis: Studi Letterari e Scientifici, Interventi di Restauro. In *Dall'Archivio Segreto Vaticano. Miscellanea di Testi, Saggi e Inventari IX*; Archivio Segreto Vaticano: Città del Vaticano, Rome, Italy, 2016; pp. 403–421.
43. Kwaśna, H.; Karbowska-Berent, J.; Behnke-Borowczyk, J. Effect of Fungi on the Destruction of Historical Parchment and Paper Documents. *Pol. J. Environ. Stud.* **2020**, *29*, 2679–2695. [CrossRef]
44. Kedves, O.; Kocsubé, S.; Bata, T.; Andersson, M.A.; Salo, J.M.; Mikkola, R.; Salonen, H.; Szűcs, A.; Kedves, A.; Kónya, Z.; et al. Chaetomium and Chaetomium-like Species from European Indoor Environments Include *Dichotomopilus finlandicus* sp. Nov. *Pathogens* **2021**, *10*, 1133. [CrossRef]

45. Wei, T.P.; Wu, Y.M.; Zhang, X.; Zhang, H.; Crous, P.W.; Jiang, Y.L. A Comprehensive Molecular Phylogeny of Cephalotrichum and Microascus Provides Novel Insights into Their Systematics and Evolutionary History. *Persoonia* **2024**, *52*, 119–160. [CrossRef] [PubMed]
46. Piñar, G.; Sterflinger, K.; Pinzari, F. Unmasking the Measles-like Parchment Discoloration: Molecular and Microanalytical Approach: Microbiota Causing Purple Spots on Parchments. *Environ. Microbiol.* **2015**, *17*, 427–443. [CrossRef]
47. Schneider, T.; Keiblinger, K.M.; Schmid, E.; Sterflinger-Gleixner, K.; Ellersdorfer, G.; Roschitzki, B.; Richter, A.; Eberl, L.; Zechmeister-Boltenstern, S.; Riedel, K. Who Is Who in Litter Decomposition? Metaproteomics Reveals Major Microbial Players and Their Biogeochemical Functions. *ISME J.* **2012**, *6*, 1749–1762. [CrossRef]
48. Eisenman, H.C.; Casadevall, A. Synthesis and assembly of fungal melanin. *Appl. Microbiol. Biotechnol.* **2012**, *93*, 931–940. [CrossRef] [PubMed]
49. Sterflinger, K. Fungi: Their Role in Deterioration of Cultural Heritage. *Fungal Biol. Rev.* **2010**, *24*, 47–55. [CrossRef]
50. Isola, D.; Bartoli, F.; Meloni, P.; Caneva, G.; Zucconi, L. Black Fungi and Stone Heritage Conservation: Ecological and Metabolic Assays for Evaluating Colonization Potential and Responses to Traditional Biocides. *Appl. Sci.* **2022**, *12*, 2038. [CrossRef]
51. Fogarty, V.; Tobin, J.M. Fungal melanins and their interactions with metals. *Enzyme Microb. Technol.* **1996**, *19*, 311–317. [CrossRef]
52. Song, W.; Yang, H.; Song, L.; Yu, H.; Li, D.; Li, P.; Xing, R. Melanin: Insights into structure, analysis, and biological activities for future development. *J. Mater. Chem. B* **2023**, *11*, 7528–7543. [CrossRef] [PubMed]
53. Afifi, H.A.M.; Mansour, M.M.A.; Hassan, A.G.A.I.; Salem, M.Z.M. Biodeterioration effects of three *Aspergillus* species on stucco supported on a wooden panel modeled from Sultan al-Ashraf Qaytbay Mausoleum, Egypt. *Sci. Rep.* **2023**, *13*, 15241. [CrossRef]
54. Mesquita, N.; Portugal, A.; Videira, S.; Rodríguez-Echeverría, S.; Bandeira, A.M.L.; Santos, M.J.A.; Freitas, H. Fungal Diversity in Ancient Documents. A Case Study on the Archive of the University of Coimbra. *Int. Biodeterior. Biodegrad.* **2009**, *63*, 626–629. [CrossRef]
55. Mazzoli, R.; Giuffrida, M.G.; Pessione, E. Back to the Past: "Find the Guilty Bug-Microorganisms Involved in the Biodeterioration of Archeological and Historical Artifacts". *Appl. Microbiol. Biotechnol.* **2018**, *102*, 6393–6407. [CrossRef] [PubMed]
56. Borrego, S.; Lavin, P.; Perdomo, I.; Gómez de Saravia, S.; Guiamet, P. Determination of Indoor Air Quality in Archives and Biodeterioration of the Documentary Heritage. *ISRN Microbiol.* **2012**, *2012*, 680598. [CrossRef]
57. Wawrzyk, A.; Rybitwa, D.; Rahnama, M.; Wilczyński, S. Microorganisms Colonising Historical Cardboard Objects from the Auschwitz-Birkenau State Museum in Oświęcim, Poland and Their Disinfection with Vaporised Hydrogen Peroxide (VHP). *Int. Biodeterior. Biodegrad.* **2020**, *152*, 104997. [CrossRef]
58. Setlow, P. Spore Resistance Properties. In *The Bacterial Spore*; ASM Press: Washington, DC, USA, 2016; pp. 201–215.
59. Michaelsen, A.; Piñar, G.; Pinzari, F. Molecular and Microscopical Investigation of the Microflora Inhabiting a Deteriorated Italian Manuscript Dated from the Thirteenth Century. *Microb. Ecol.* **2010**, *60*, 69–80. [CrossRef]
60. Borrego, S.; Guiamet, P.; Vivar, I.; Battistoni, P. Fungi Involved in Biodeterioration of Documents in Paper and Effect on Substrate. *Acta Microsc.* **2018**, *27*, 37–44.
61. Fouda, A.; Abdel-Nasser, M.; Khalil, A.M.A.; Hassan, S.E.-D.; Abdel-Maksoud, G. Investigate the role of fungal communities associated with a historical manuscript from the 17th century in biodegradation. *npj Mater. Degrad.* **2022**, *6*, 88. [CrossRef]
62. Nitiu, D.S.; Mallo, A.C.; Saparrat, M.C.N. Fungal Melanins That Deteriorate Paper Cultural Heritage: An Overview. *Mycologia* **2020**, *112*, 859–870. [CrossRef]
63. Voříšková, J.; Baldrian, P. Fungal Community on Decomposing Leaf Litter Undergoes Rapid Successional Changes. *ISME J.* **2013**, *7*, 477–486. [CrossRef] [PubMed]
64. Florian, M.-L.E. *Fungal Facts: Solving Fungal Problems in Heritage Collections*; Archetype Publications: London, UK, 2002.
65. Tláskal, V.; Voříšková, J.; Baldrian, P. Bacterial Succession on Decomposing Leaf Litter Exhibits a Specific Occurrence Pattern of Cellulolytic Taxa and Potential Decomposers of Fungal Mycelia. *FEMS Microbiol. Ecol.* **2016**, *92*, fiw177. [CrossRef] [PubMed]
66. Pan, X.; Raaijmakers, J.M.; Carrión, V.J. Importance of Bacteroidetes in Host-Microbe Interactions and Ecosystem Functioning. *Trends Microbiol.* **2023**, *31*, 959–971. [CrossRef] [PubMed]
67. Baldrian, P. Forest microbiome: Diversity, complexity and dynamics. *FEMS Microbiol. Rev.* **2017**, *41*, 109–130. [CrossRef]
68. Wang, C.; Kuzyakov, Y. Mechanisms and Implications of Bacterial-Fungal Competition for Soil Resources. *ISME J.* **2024**, *18*, wrae073. [CrossRef]